Relativistic Klystron Two-Beam Accelerator Approach to Multi-TeV e^+e^- Linear Colliders*

S.M. Lidia[a], T.L. Houck[b], G.A. Westenskow[b], and S.S. Yu[a]

[a]*Lawrence Berkeley National Laboratory, One Cyclotron Road, Berkeley, CA 94720*
[b]*Lawrence Livermore National Laboratory, P.O. Box 808, Livermore, CA 94550*

ABSTRACT

We propose a design for a multi-TeV electron-positron collider based on the relativistic klystron two-beam accelerator (RK-TBA) concept. Given the source requirements from a particle physics perspective, we discuss the intersection of interaction point (IP), linac, and RF power source physics that influence our choice of parameters. In particular, we examine a possible design with a 5-TeV center-of-mass energy. We show that operation of an RK-TBA at 30 GHz with a wall-plug to high-energy-beam power conversion efficiency of 50% could be possible, subsequent to advances in design and fabrication of heavily damped RF structures. We discuss the issues surrounding high efficiency power production, and the transfer of power from beam to beam. Issues of beam dynamics in both linacs are addressed.

I. INTRODUCTION

The relativistic klystron two-beam accelerator scheme [1] presents a highly efficient source of high power microwaves for collider applications at frequencies up to approximately 35 GHz. This upper frequency range is appropriate for driving high gradient structures in a multi-TeV linear collider, where accelerating gradients over 100 MeV/m are desired. Our original design proposal considered an RK-TBA power source at 11.424 GHz for a 1-TeV collider. This paper presents a possible design for a 5-TeV collider power source operating at 30 GHz. Since we assume heavy damping in the RF structures, we call this design HD-TBA.

Because of the intrinsic high efficiency of the RF power production process, we adopt a somewhat different strategy in the collider design. In particular, we propose the use of high current, high power beams in the main collider linacs, while loosening some of the stringent parameters in the final focus section. We will discuss our choice of interaction point (IP) parameters in section II, and compare them with other collider proposals. In section III, we consider the high gradient structures using design tools that emphasize power conversion efficiency of RF to beam. The relativistic klystron itself is presented in section IV, along with a discussion of the system efficiencies.

*This work was performed under the auspices of the U.S. Department of Energy by LBNL under Contract No. AC03-76SF00098, and by LLNL under Contract No. W-7405-ENG-48.

II. INTERACTION POINT PHYSICS

In this section we discuss the constraints imposed by the beam-beam interaction at collision that affect the choice of parameters in the main linac transport and final focus sections. For a definition of terms and a comprehensive review of the relevant IP physics in a linear collider, we refer to Wilson [2], Palmer [3], and Irwin [4].

Requirements of high average luminosity, a usable level of beamstrahlung induced energy spread, and a low background of high energy photons lead to tradeoffs between beam power and beam quality. The NLC [5] klystron-based collider designs have exhibited overall wall plug to beam efficiencies around 10%. In order to hold down total power consumption, a heavy burden is usually placed on generating and maintaining higher quality beams, keeping the beam power at lower levels. In this HD-TBA collider design, the net efficiency can be 50% or more. In this scheme, we choose instead to operate with much higher beam power in order to relax some of the constraints and challenges at the final focus. Various proposed schemes, and their IP parameter sets are listed in Table I. The parameters of the 1-TeV NLC case are included for comparison.

Table I: Comparison of linear collider IP parameters.

	Palmer [3]	Irwin [4]	Wilson [2]	HD-TBA**	NLC [5]
E_{cm} (TeV)	5.0	5.0	5.0	5.0	1.0
$L(10^{35}cm^{-2}s^{-1})$	2.5	2.5	2.5	2.5	0.11
$N(10^{10})$	0.31	0.03	0.44	0.25	1.1
$f_{rep}n_b$(kHz)#	12.7	330	5.6	71	12.6
σ_y(nm)	0.2	0.1	0.1	0.4	5.1
R	136	156*	700	180	49
$\sigma_z(\mu m)$	20	27*	20	20	150
ε_{ny}(nm)	1.5	3.3	1	4	110
D_y	7.3	7	7	2	7.6
H_D	2	1.4*	1.1*	2	1.4
Υ	21	4*	28	7.8	0.29
δ_B(%)	27	10*	20	15.5	12.6
P_{beam} (MW)	54	40	18	72	7.9

* These parameters are not given explicitly by the authors, but have been derived from scaling relationships.
** We have used a value of A_y equal to 0.10.
# f_{rep} is the pulse train repetition frequency; n_b is the number of bunches per train.

For the RK-TBA design we have allowed for both a larger beam spot size and normalized emittance, while keeping Υ and δ_B at moderate values. The range of Υ considered in the various designs spans an order of magnitude. The physics of high (>>1) Υ interactions is still not understood, so placing any upper limit is somewhat premature. Also, the issue of energy resolution in the detector systems must be addressed before an upper limit on δ_B can be imposed as a design constraint. However, in a reasonable 5-TeV collider design, it is very difficult to achieve an energy spread below 10%. Extending to 20% or more is desirable as it would allow the final focus constraints to relax.

This loosening of beam quality does not come without its price. The RK-TBA RF power source is most efficient when generating long RF pulses (100's to 1000's of ns). Efficient use of that pulse means that we must use bunch trains that span it. To achieve the required luminosity, we must also pack the bunches tightly together. The current HD-TBA design uses trains of 4761 0.4 nC bunches with a separation of 2 RF wavelengths. This gives a large DC current of 6.01 A during the pulse. However, we need only pulse the system at a repetition rate of 10 Hz.

III. HIGH GRADIENT STRUCTURES

The transport and acceleration of such large current beams necessitates a hard study of the high gradient structures. See the introduction by Wilson [6] for a discussion of the pertinent physics. A detailed calculation of the structure parameters proposed has not yet been done, but will be required in a more detailed study.

Once an average current is chosen, the structure design becomes a tradeoff between accelerating gradient and RF to beam power conversion efficiency. Here, we adopt an approach that uses heavy beam loading to boost efficiency, while maintaining relatively high loaded accelerating gradients. We assume that the high gradient structures operate in the $2\pi/3$ mode, and can be modeled with a constant impedance along their length. The conversion efficiency of RF to beam power in the structure can then be studied as a function of attenuation (τ) and the ratio Gmin/G0. This is shown in Figure 1. Here G0 is the gradient at the front end of the structure, while Gmin is the gradient at the downstream end. The square of the ratio Gmin/G0 gives the fraction of input power which flows into the matched load at the downstream end.

A complementary view of this process is shown in Figure 2. There we plot the conversion efficiency (solid, percentages) and the average loaded gradient per input gradient (Gavg/G0) (dotted, decimals) as a function of attenuation (τ) and beam loading (Idc·r / G0). Here Idc is the beam DC current, and r is the longitudinal shunt impedance per unit length in the structure.

Figure 1: RF to beam conversion efficiency.

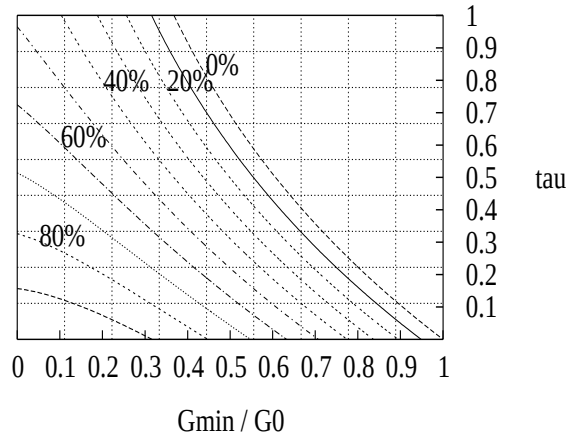

These charts are useful for the design process once a DC current is chosen. We match efficiency with structure length and attenuation (τ), and longitudinal shunt impedance (r). Then, choosing the average loaded gradient (Gavg) determines the input gradient (G0), and thus the required input power. Together, these two plots are used to design a self-consistent structure, in combination with well-known scaling laws of $2\pi/3$ structures [7].

Figure 2: Power conversion efficiency and loaded gradient.

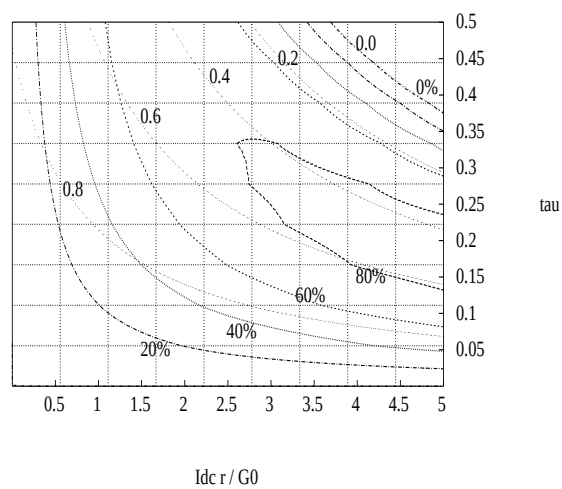

The linac structures are designed to have high efficiency in transfer of RF power to beam power (~80%), with high input RF power (400 MW/structure). Heavy beam loading then requires that the structure walls absorb the remaining power. This amounts to 80 MW per 300 ns pulse, but the pulses have a low repetition rate (10 Hz), so that the average power absorbed is 240 W. Damage to the structure incurred by surface heating must still be examined. The structure parameters are listed in Table II.

Table II: Linac structure parameters.

Frequency	30 GHz	Idc	6.01 A
βgroup	0.10	P0	400 MW
a/λ	0.214	G0	244 MV/m
r/Q	23.7 kΩ/m	Gavg	126 MV/m
Q	4425	Pbeam/P0	0.79
Fill time	14 ns	Pwall/P0	0.20
τ	0.298		

The transverse wakefields in this structure are quite severe due to the large current. By using heavily damped structures, such as those employing waveguides to transport the higher order modes away from the beam, in addition to detuning the cells, we can produce designs with low dipole mode Q's [8]. This can significantly damp wakefield levels generated by a bunch at a given point in the structure by the time the next bunch arrives. Detailed simulations of the beam dynamics in this environment are beyond the scope of the present paper, but will need to be performed in a more thorough study.

IV. RELATIVISTIC KLYSTRON SOURCE

The relativistic klystron power source design is similar to the proposed TBNLC [9], which would generate 360 MW/m at 11.424 GHz. The main layout is depicted in Figure 3. For this design, each unit would power 600 high gradient structures, so that each linac arm would require 79 HD-TBA units.

Each HD-TBA consists of a 3.5 kA, 5.0 MeV injector, a beam modulation unit, an adiabatic capture section to bunch and accelerate the beam, the main RF extraction section, and an afterburner section to extract power from the beam while decelerating it prior to the dump. At the entrance to the main extraction section, the beam has an average energy of 25 MeV and carries 3150 A of RF current with 1750 A of DC current.

Figure 3: HD-TBA Unit Layout.

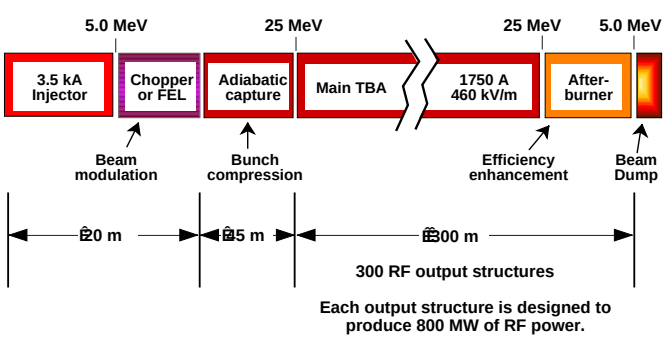

A 1-m long repeating unit of the main extraction section is shown in Figure 4. Each relativistic klystron has 300 of these sections to power 600 high gradient structures.

The ultimate efficiency of the relativistic klystron is limited by the number of extraction sections the beam can pass through before succumbing to beam breakup (BBU) instabilities. Careful attention must then be paid to transport and stability.

Figure 4: HD-TBA Extraction Section.

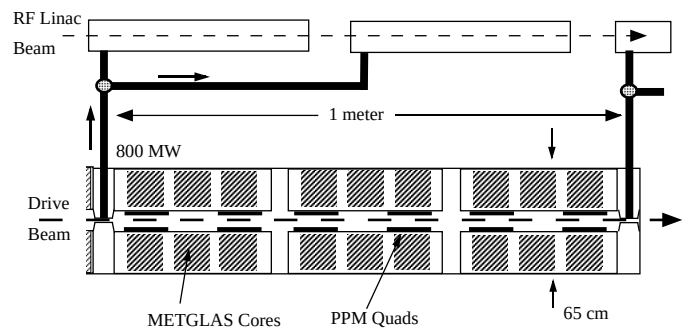

A. Transport and Beam Stability

Permanent magnet quadrupoles are employed to provide the magnetic FODO lattice. The lattice has a 0.33 m period with a 60° phase advance per period, giving a 2 m betatron period. The quadrupole magnets are ferrites with an 800 G pole field, 1.0 cm bore radius, and 0.48 occupancy factor. For a normalized edge emittance of 2000π mm-mrad, the equilibrium beam edge radius will be about 2.0 mm. This emittance requirement can be relaxed somewhat, since the output structure apertures have a radius of 3 mm, but a high emphasis must be placed on the generation and preservation of low emittance beams.

Two severe transverse instabilities have been identified in the RK-TBA. One is a low frequency mode associated with the induction modules, and the other is a high frequency mode due to the RF extraction structures. Similar instabilities will exist in this design, but at concomitantly higher frequencies. Simple scaling arguments [10] of the dependence of the transverse impedance to changes in frequency and structure parameters, as well as changes in the beam energy and DC current imply that the high frequency instability growth rate in this design could be a factor of 4 higher than in the TBNLC design, while the low frequency instability rate could be 10 times higher, if left uncorrected.

Energy spread in the beam should result in effective Landau damping to counter the low frequency instability. Transport of the beam depends upon the ferrite permanent magnet quadrupoles. By increasing the poletip field of the magnets, the quadrupole gradient on-axis will also increase. Alternatively, we can increase the bore of the beam pipe as well as induction gaps, while increasing the poletip field at fixed beam energy, and maintain the same betatron period. Thus, we can decrease the transverse impedance due to the induction gaps, and hence the low frequency instability growth rate.

Another beam dynamic issue related to the induction cell is the extraction of RF power from the modulated beam. This power is absorbed by various materials in the cell and reduces efficiency. Techniques for lowering the longitudinal

impedance of the cell at 30 GHz, therefore minimizing power loss in the output strucures, is an active area of study.

The higher frequency mode is more severe. Our solution is to place the extraction structures at half-betatron wavelengths, on the nodes. The growth rate should be similarly depressed as in the betatron node scheme for the TBNLC [11]. Field error tolerances in the quadrupoles become an issue, since this instability is sensitive to the details of the focusing lattice with respect to the positions of the RF output structures.

A transverse chopper or an FEL can used to modulate the 5-MeV beam at 30 GHz. The initial bunch length initially spans 240° of longitudinal phase. The adiabatic capture section then compresses the bunches so that they occupy 70° of phase by the time they enter the main RK-TBA extraction section. Also, if an FEL is to be used, the DC current produced by the injector can be lowered substantially, since all of the beam can theoretically be bunched. This is in contrast to modulation by the chopper, where half the beam is lost.

The idler cavities in the adiabatic capture section and the extraction structures in the main section are detuned from synchronism at 30 GHz. This compensates for bunch lengthening effects, and provides longitudinal focusing. The synchrotron oscillation, induced by the power extraction and reacceleration, has a period of 91 m.

B. Travelling Wave Output Structures

The proposed 30 GHz output structure is shown in Figure 5. We obtain a zero-order design by scaling the physical dimensions of the structure from our 11.424 GHz design. The structure is initially designed to operate in the $2\pi/3$ mode, but is then detuned by 30° so that it will actually resonate in the $\pi/2$ mode when driven at 30 GHz. The travelling wave then has a phase velocity of 1.33c. We derived scaling laws from numerical simulations of $\pi/2$ mode structures so that we can accurately model the longitudinal impedance as the iris aperture changes.

Figure 5: Travelling Wave Output Structure.

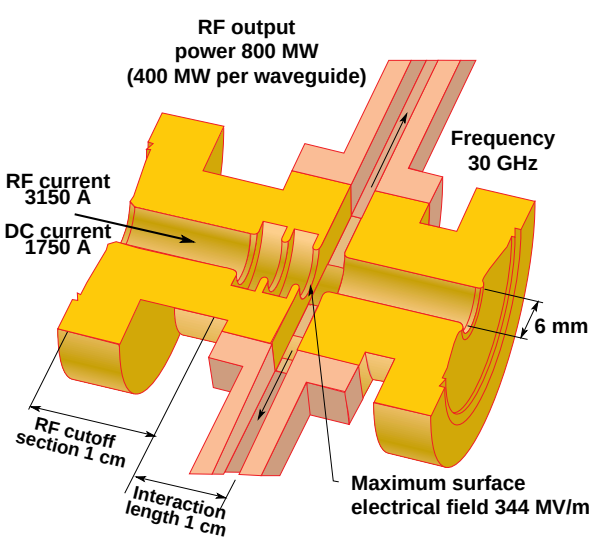

We find the appropriate longitudinal shunt impedance which will allow our beam to produce 800 MW, by opening the iris so that the group velocity of the mode is approximately 0.65c. With a field enhancement factor of 1.5, we then expect the maximum surface fields to be 344 MV/m. The structure parameters are listed in Table III.

Table III: Travelling wave output structure parameters.

Frequency	30 GHz	R/Q	19 Ω/cell
Mode	$2\pi/3$ *	Pout	801 MW
βgroup	0.65	Max field	344 MV/m
a/λ	0.62		

* Detuned by 30° - resonant travelling mode is $\pi/2$.

Dipole modes exist in this structure giving rise to the severe high frequency BBU instability mentioned earlier. We are currently evaluating choked mode cavity designs [12] to decrease the transverse impedance. Other schemes are also possible to decrease impedance, or the instability growth rate. The betatron node scheme has already been mentioned.

C. Induction Modules

We have designed a system to provide 155 kV per induction cell, to replace the beam energy lost in the RF output structures. For the core material we currently have three choices: Ceramic Magnetics CMD-5005 ferrite (ΔB~0.65T), Allied-Signal METGLAS 2605SC (ΔB~2.50T), and METGLAS 2714AS (ΔB~1.10T). Each have different properties that make them superior to the others in different regimes of voltage and pulse length. For our long pulse (300 ns), and assuming that we drive the core to saturation, the 2714AS material has the lowest losses, and hence the largest efficiency.

Figure 6: Core Efficiencies.

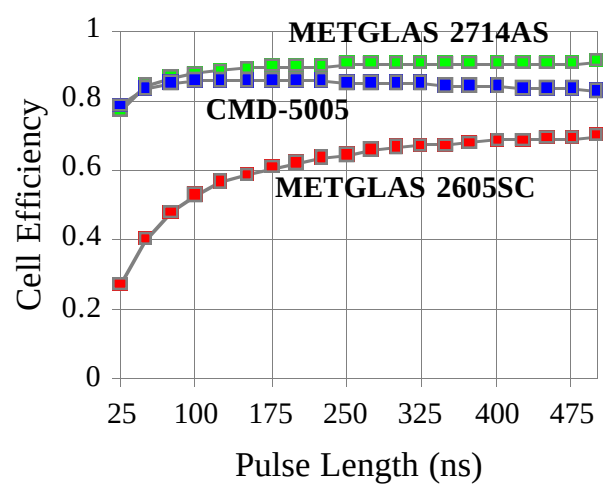

For a DC current of 1750 A and voltage of 155 kV/cell, the net core efficiency is ~91%. The core efficiencies for these materials are plotted versus pulse length in Figure 6. This

high efficiency design must be balanced against cost, since the core volume increases rapidly with pulse length.

D. System Efficiencies

The pulse power system suitable for this design would utilize a DC power supply, a command resonant charging (CRC) chassis, and thyratron switching, like the earlier TBNLC proposal. We can make predictions of the efficiency of the pulse power system based on our previous work. These estimates are listed below in Table IV. Here the drive beam fall time has been included to account for losses at the end of the voltage pulse that are dissipated in the induction cores. Drive beam to RF losses account for the beam losses at the front end of the relativistic klystron, and for beam power lost at the dump. Auxiliary power accounts for cooling and vacuum systems, etc. We include the RF to beam efficiency of the high gradient structures, and calculate the net efficiency of the RK-TBA to be ~52%.

Table IV: Power source efficiencies.

DC Power	0.93
CRC	0.96
Modulator (Thyratron)	0.94
Induction Cells	0.91
Drive Beam (Fall Time)	0.94
Drive Beam to RF	0.93
Auxiliary Power	0.98
RF to High Energy Beam	0.79
Net Wall Plug to Beam	0.52

V. SUMMARY

We have presented a design for a 5-TeV collider based on the relativistic klystron two-beam accelerator scheme. We have shown that an efficient power source can alleviate some of the more stringent requirements on the high energy beam quality and final focus system. In particular, high efficiency allows the use of larger beam spot sizes and normalized emittances at the IP. We have identified possible problems in the RF structures that require more careful study. We have discussed the operation of the relativistic klystron, and shown that highly efficient generation of nearly a gigawatt of RF power per meter at 30 GHz can be possible.

VI. ACKNOWLEDGMENTS

We gratefully acknowledge David Anderson, Swapan Chattopadhyay, Shmuel Eylon, Enrique Henestroza, Jin-Soo Kim, Andrew Sessler, and Ming Xie for useful discussions.

VII. REFERENCES

[1] Houck, T., ed., "An RF Power Source Upgrade to the NLC Based on the Relativistic-Klystron Two-Beam Accelerator Concept," Appendix A of the *Zeroth-Order Design Report for the Next Linear Collider*, SLAC Report 474, Stanford University, Stanford, CA, May 1996.

[2] Gaponov-Grekhov, A.V., and Granatstein, V.L., eds., *Applications of High Power Microwaves*, Boston: Artech House, 1994, ch. 7.

[3] Palmer, R.B., *Ann. Rev. Nucl. Sci.* **40**, 529-92 (1990).

[4] Irwin, J., "Bird's IP View of Limits of Conventional e+e- Linear Collider Technology," presented at the 6th Workshop on Advanced Accelerator Concepts, Lake Geneva, Wisconsin, June 12-18, 1994.

[5] The NLC Design Group, *Zeroth-Order Design Report for the Next Linear Collider*, SLAC Report 474, Stanford University, Stanford, CA, May 1996.

[6] Wilson, P., SLAC-PUB-2884 (rev.) (1991).

[7] Farkas, Z.D., "The Roles of Frequency and Aperture in Linear Accelerator Design," in *Proceedings of the 1988 Linear Accelerator Conference*, Williamsburg, VA, October 3-7, 1988, pp. 583-585.

[8] Lin, X.E., and Kroll, N.M., "Minimum Wakefield Acheivable by Waveguide Damped Cavity," in *Proceedings of the 1995 IEEE Particle Accelerator Conference*, Dallas, TX, May 1995, pp. 1809-11.

[9] Yu, S.S., et. al., "Relativistiv-Klystron Two-Beam Accelerator Based Power Source for a 1 TeV Center-of-Mass Next Linear Collider - Preliminary Design Report," UCRL-ID-119908 (1995).

[10] Chao, A.W., *Physics of Collective Instabilities in High Energy Accelerators*, New York: John Wiley & Sons, 1993.

[11] Giordano, G., et. al., "Beam Dynamics Issues in an Extended Relativistic Klystron," in *Proceedings of the 1995 IEEE Particle Accelerator Conference*, Dallas, TX, May 1995, pp. 740-42.

[12] Shintake, T., *Jpn. J. Appl. Phys. Lett.* **31**, 1567 (1992).